NORMALIZED SECOND-ORDER STATISICS FOR TEXTURE CHARACTERIZATION

by

CHARMAINE JOY-ANNE OKOLO HARRIS
B.S. Bethune-Cookman College, 1996

A thesis submitted in partial fulfillment of the requirements
for the degree of Master of Science
in Department of Optical Sciences and Engineering, in the College of Engineering
at the University of Central Florida
Orlando, Florida

Spring Term
1999

ABSTRACT

The science of texture analysis is fundamental to various applied fields such as medical diagnosis, remote sensing, and material science. Recently, it has been proposed that the normalized complete second-order statistics, also referred to as the two-point probability density function (2P-PDF), be used for texture characterization.[12] This conjecture is supported by Julez's 1962 visual experiments which showed that the human visual system could not discriminate textures of equal first- and second-order statistics.[7]

The aim of this research is to investigate class separability for classification efficacy based on different normalization schemes of 2P-PDFs. Three different methods of normalization were considered: linear scaling, and matching of first-order statistics to either a uniform or a Gaussian distribution.

Considering four visually discriminable texture ensembles, results show that matching to an image with a Gaussian grey level distribution provides the highest level of class separability. The two other normalization schemes considered, linear scaling and the matching of first-order statistics to a uniform distribution, yield a good but sub-optimal and a poor class separability, respectively. Based on the results of matching first-order statistics to a Gaussian distribution, this normalization method will be next tested across medical imaging data sets that typically offer more subtle differences.

To: Veron, Ohene, Beverly, and Olive.

ACKNOWLEDGEMENTS

I would like to acknowledge and thank my advisor, Dr. Jannick Rolland, for her guidance and patience throughout my studies in graduate school. Her support and understanding are greatly appreciated. I would like to thank Alexei Goon for his technical contributions to this work, and for the additional help that he willingly provided. I would also like to thank Brian Bloss for his assistance in the programming that was necessary to perform this work. Additionally, I wish to thank Larry Davis and Yann Argotti for the many questions that they have answered and the help that was readily offered. Finally, I would like to thank my family for their love, support, and encouragement.

This work was in large supported by an Office of Naval Graduate Fellowship. It was also supported in part by a 1997 Florida I4-Corridor Award.

TABLE OF CONTENTS

Page

LIST OF FIGURES

Figure Page

LIST OF TABLES

CHAPTER 1 - INTRODUCTION

The research presented in this thesis describes the use of normalized second-order grey level statistic as a basis for effective texture characterization. While its application to medical imaging is ultimately our aim, the methods apply generally across various fields of image science as well.

Medical imaging is an assistive technique in the diagnosis of various illnesses. It is required that medical images be of good quality in order for the technique to be effective. This leads to the need for image quality criteria and assessment. Image quality assessment is the ability to extract useful information from an image, for medical or scientific purposes. It can also be defined as the ability of a human or a mathematical model "observer" to perform a task. Task performance in medical diagnosis can be split into two categories, classification and estimation tasks.[1]

There are, however, certain problems associated with the use of different observers. For example, psychophysical methods that can be utilized to quantify task performance of a human observer do not provide in themselves a direct relationship between the image quality and the optimal setting of the imaging system or parameters of the processing algorithm. Additionally, these studies are tedious and time consuming. Finally, given the diversity in the type of images (e.g. fatty breast mammograms versus dense parenchyma), large numbers of images are required.[2]

To alleviate the problems associated with psychophysical studies, mathematical models could be utilized as predictors of human performance, and researchers strive to establish such models.[20] Ideally, such models require the determination of the grey level statistics of the image backgrounds, the model of the imaging system or the parameters of the algorithm, and the characterization of the signal to be extracted.

Beginning with the grey level statistics of the image backgrounds, a complete description of the associated probability densities must be determined. However, in many practical cases a complete knowledge of the probability densities is neither readily available nor feasible to calculate.[3] An alternative is to utilize a model that only requires the use of partial grey level statistics such as the first- and second-order statistics. Upon doing so, it is necessary to estimate the grey level statistics with the use of a group of similar images, referred to as an ensemble of images.

In remote sensing, an ensemble of images (e.g. images of a wheat field) can be obtained by a series of pictures taken of a type of agricultural environment. Such an ensemble of images forms a class. In the case of medical data sets where the images may vary on a continuum from patient to patient, thus offering no specific evidence of where one class ends and another begins, another technique is to apply a texture synthesis algorithm to an image. This technique allows synthesis of an ensemble of images, in order to form a class. Another approach may consist of gathering a time sequence of images for a particular patient diagnosed as normal according to standard procedures. This time sequence could be made over a span of months or years. Such an ensemble of images whose grey level statistical properties may be estimated would characterize the

class "normal" for that patient. An image acquired at a latter time whose grey level statistical properties differ significantly from those established for the class "normal" may suggest a state of illness.

The modeling of the imaging system is completed through the understanding and application of the physics of the imaging process. Lastly, the characteristics of the signal to be extracted are specified by the task. An example of a detection task would be a radiologist looking for tumors ranging in size from 1 mm to 10 mm and having different borders. For a texture classification task, the desired signal of interest is the texture itself. An example would be the diagnosis of liver disease, comparing an abnormal liver ultrasound to a normal liver ultrasound.[4] Classification is also applicable to many areas outside the medical field. Two such fields are material science, for rock classification; and remote sensing, for habitat determination.[5]

The research presented here deals with texture characterization, for the problem of image classification. Characterization of texture images deals with the statistical grey level description and definition of sets of distinct texture classes, whereas classification is the grouping or distribution of samples to the appropriate class. Due to the wide applicability of texture analysis in image understanding, improvements in the characterization process are desirable. We propose to characterize texture classes based on their complete second-order grey level statistics.

The research is presented in three main chapters: Chapter 2 describes the basis for the normalization of the second-order grey level statistics and an associated distance measure. The experimental methodology that acts as the basis for image simulation and

modification, as well as the distance measure are given in Chapter 3. Finally, the results of the distance measures within and between classes are presented in Chapter 4.

CHAPTER 2 – A MEASURE OF TEXTURE CHARACTERIZATION BASED ON SECOND-ORDER STATISTICS

2.1 Second-order statistics

An image such as a texture can be considered to be a two-dimensional random process. Second-order grey level statistics of a random process can be defined as the ensemble two-point probability density function (2P-PDF). Given two pixels separated by a distance vector $\mathbf{r} = \mathbf{r}(x,y)$ shown in Figure 1 the 2P-PDF of an ensemble of texture images is defined as the probability of co-occurrence of the associated grey levels when observed over the ensemble of texture images, and as $\mathbf{r}$ varies in length and orientation.

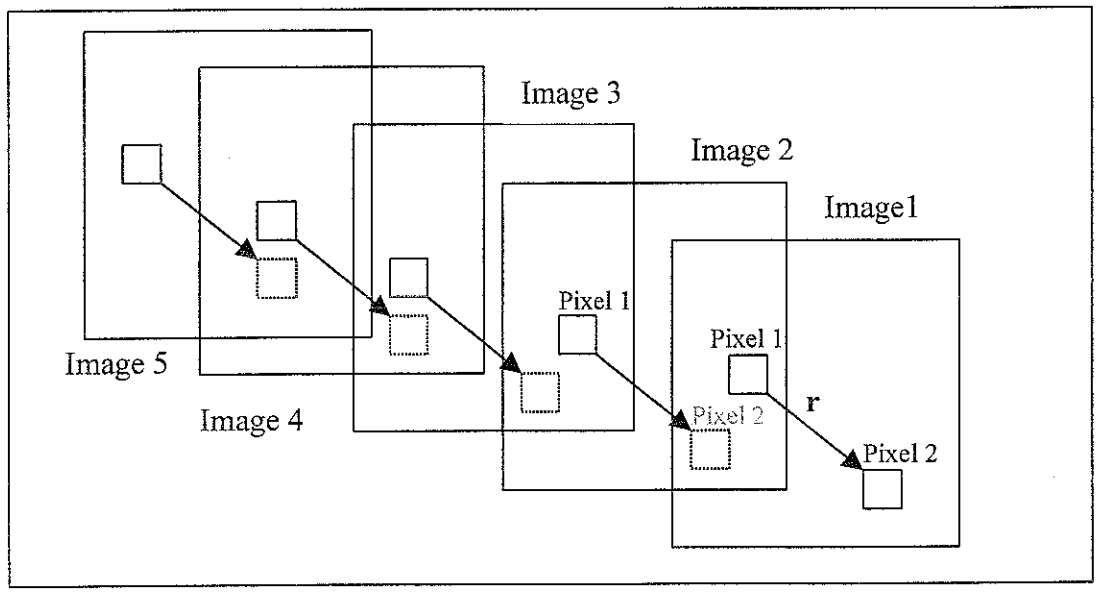

Figure 1 The complete 2P-PDF is illustrated. Given a vector **r** that separates two pixels of potentially different grey levels, the 2P-PDF determines the frequency of occurrence of the pair of grey levels throughout an ensemble of texture images. As **r** varies in length and orientation the complete 2P-PDF is formed.

The 2P-PDF provides structural information about a random process, as it offers information on the spatial relationship between grey levels at multiple scales and orientations. The 2P-PDF can be determined for either an ensemble of texture images or for an individual texture image. An example of a 2P-PDF for a particular scale and orientation is shown in Figure 2. The 2P-PDF is a graphical description of the co-occurrence of grey level pairs. The ensemble 2P-PDF is determined as depicted in Figure 1. For an individual texture image, the 2P-PDF of a given scale and orientation is calculated by determining the grey level distribution of all pixel pairs within the image that are separated by a vector distance **r**. As **r** varies in scale and orientation, the 2P-PDF is formed.

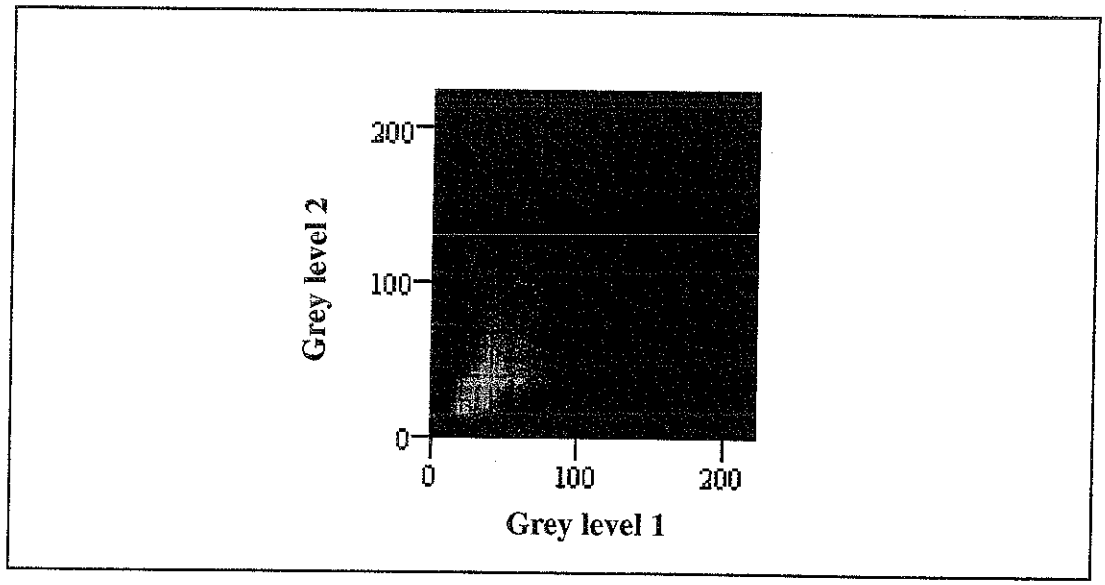

Figure 2 The 2P-PDF is plotted. For a specified vector **r** the co-occurrence of grey level values 1 and 2 is plotted. The lighter colors represent a higher frequency of occurrence of grey level pairs.

This concept can also be understood by observing the joint probability distribution function of two grey levels given by

$$P(g_1,g_2) = P(g_1)P(g_2|g_1), \quad (1)$$

where $P(g_1)$ is the one-point probability density function (1P-PDF), i.e. the distribution of grey levels within an image, and $P(g_2|g_1)$ is the conditional probability density of grey level g_2 occurring given that grey level g_1 has occurred. Thus we are able to not only determine the probability of the grey level value of a given pixel, but we are also able to determine the probability of the grey level value of that pixel with respect to the grey level value of another pixel. It is also important to note that g_1 and g_2 are considered to be statistically independent if the occurrence of one pixel has no bearing on the occurrence of the other. In this case it follows that

$$P(g_1,g_2) = P(g_1)P(g_2|g_1) = P(g_1)P(g_2). \quad (2)$$

Eq. 2 expresses that if the two random variables are uncorrelated, their joint probability density function becomes the product of the two marginal density functions, or 1P-PDFs.[6] This observation will be shown to be the basis for the contribution of the research presented here.

2.2 Why Use Complete Second-Order Statistics?

We shall motivate answers to why we propose to use complete second-order statistics as a basis for characterization, instead of extracted features from second-order statistics. This can be addressed by giving an example of the use of an extracted feature. The power spectrum, for example, which is one component of the complete second-order

statistics, is often considered for texture characterization.[8] The power spectrum of a stationary random process is defined as the Fourier transform of the process' autocorrelation function. In many cases the justification for its use is that power spectrum analysis has been a means of spectral analysis of noises and other signals. However, the use of the power spectrum does not provide sufficient information for texture image characterization because texture images have more complex structures.

The inability of the power spectrum to offer adequate information, when pertaining to a statistical texture, is based on the fact that the power spectrum only retains amplitude information while disregarding phase information. Since the phase characteristics specify the structural information of an image, the power spectrum does not provide a unique description of the image.[9,10] Consequently there may be multiple texture images with the same power spectrum but potentially having different structural makeups, thus nullifying the ability of the power spectrum to provide an accurate basis for texture characterization in many cases. Only in the case of a Gaussian random process does the power spectrum provide enough information to completely describe the second-order statistics. Hence for non-Gaussian processes the power spectrum only provides a portion of the descriptive information necessary for the complete description of the second-order statistics.

Yet another question to be addressed is, "Why not use higher-order statistics?" Based on Julez' experiments, it is known that visual discrimination between images with the same first- and second-order statistics is not possible.[7] Thus when dealing with texture images with differing second- and higher-order statistics it is a worthwhile step to

first look at the complete second-order statistics before delving into higher-order statistics. Higher-order statistics may be considered as a basis for future work, depending on whether the complete second-order statistics are capable of fully characterizing texture images. Thus, in the endeavor to acquire an effective figure of merit for complex background characterization, we propose to use the complete 2P-PDF.[1,19]

2.3 Texture synthesis

The estimation of the two-point probability density function most generally requires that an ensemble of statistically equivalent texture images be provided. To synthesize an ensemble of images, we utilize a texture synthesis algorithm previously developed by Rolland et. al.[11] The texture synthesis framework employs a recursive steerable pyramid transform which has a set of filter banks. The pyramid transform consists of four layers each providing filtering of the sample texture images and downsampling by a factor of two. The filtering is made by bandpass and orientation filters. The orientation filters form a quadrature mirror filter bank.[11] The texture image is decomposed by feeding it through the pyramid transform. In parallel, a uniformly distributed white noise image is also input into the pyramid transform. The white noise image acts as a point of origination for the synthesis. Once the decompositions have been completed, the histograms of the white noise image are matched to that of the sample image at multiple scales and orientations. To compute the synthesis, the histogram-matched noise images acquired at each orientation and scale are recombined, in a bottom up recombination process. A factor of two upsampling and Gaussian blur are applied

between scales, during recombination. Loss of brightness, due to the downsampling, is also accounted for at this time. The process is iterated to yield a synthetic image. To create another synthesized image a different realization of white noise must be employed.

2.4 Texture characterization

When performing texture classification there are two main concerns to be addressed: the definition of the classes and the classification criteria. The former, referred to as texture characterization, is most important. The efficacy of classification is dependent upon how distinct the classes are, which in our case will be specified by a distance metric between the 2P-PDFs.[12] Standard classification methods can always be applied.

2.4.1 Definition of classes

To define the various classes, the boundaries of the spread of textures within a class must first be determined. Each realization of a texture within a class has an estimated 2P-PDF associated with it, as does the texture ensemble. For each texture a distance d can be computed between its 2P-PDF and the average 2P-PDF of the ensemble. Therefore, there is a probability distribution P{d} associated with d, over the texture ensemble. The associated cumulative distribution function can be computed as

$$C_d(\mathbf{r}) \equiv P\{d \leq \mathbf{r}\}, \qquad (3)$$

the probability that the distance between the 2P-PDF of a texture and the ensemble average 2P-PDF is less than or equal to some parameter **r**. The cumulative distribution

function has a value between zero and one. The radius of a class can now be defined as the value of **r** at which a specific value of the cumulative probability distribution function (CPDF) is achieved.[13] For example, if the value of the CPDF is .95, then the radius of some class C is expressed as, r^{C}_{95}. Using the 2P-PDF of a texture ensemble, the radius of a texture class can thus be determined.

The determination of how close two classes are, is also a significant issue. An effective measure of classification requires that the distance between two classes, let us call them A and B, be greater than the sum of the two radii of the associated classes,

$$d_{AB} > r^{A}_{.95} + r^{B}_{.95}. \qquad (4)$$

This is represented Figure 3. This example provides a maximum response, however the classification error will vary depending on how much overlapping occurs between the two texture classes. For example, if

$$r^{B}_{.95} > d_{AB} + r^{A}_{.95} \qquad (5)$$

then it follows that a complete discrimination between the two classes is not possible, since class A is within class B, as depicted in Figure 4.

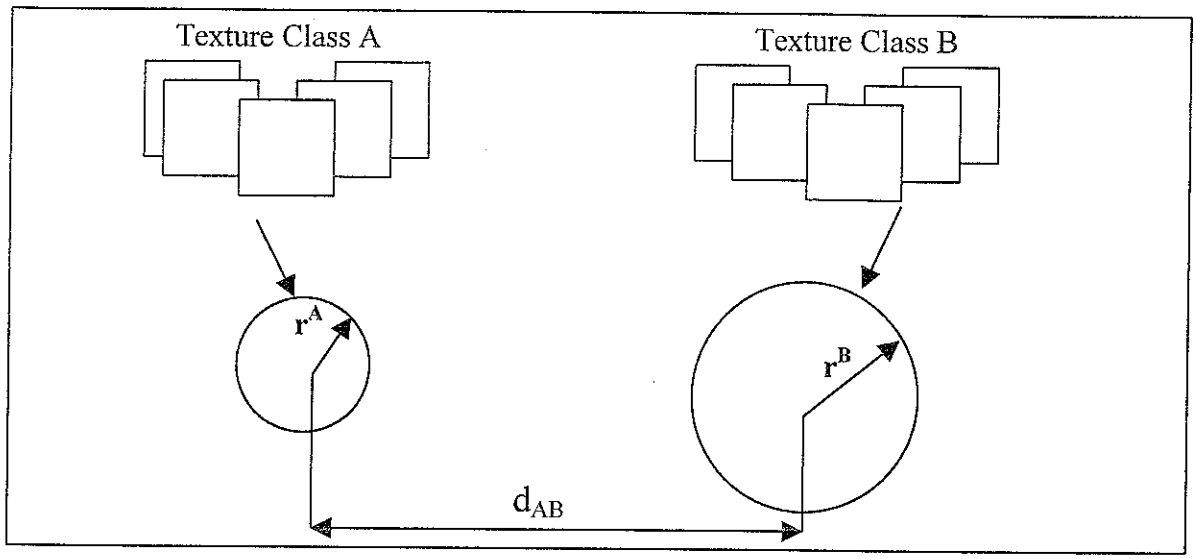

Figure 3 The complete discrimination between two texture classes is illustrated. Given two texture classes A and B, the ability to discriminate between the two classes is dependent upon the distance d_{AB} between the two classes being greater than the sum of the radii of the individual classes, $r^A_{.95} + r^B_{.95}$.

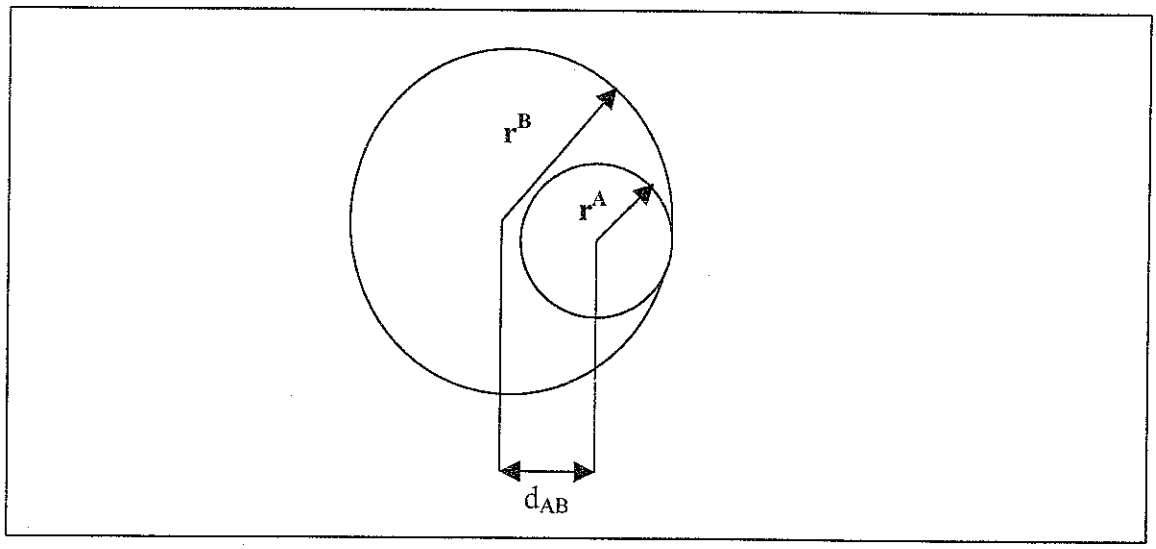

Figure 4 The total lack of discrimination between two texture classes A and B is illustrated. Since the distance between the two classes d_{AB} is less than the sum of the radii of the classes, no discrimination between the classes is possible.

2.4.2 Distance measure

The quantification of class separability can now be undertaken, given that the spread of textures within the classes has been defined. The method of class separability we propose is based on the quantification of the similarity between two 2P-PDFs. A distance measure between two texture classes A and B can be established by calculating the root-mean-square distance between two probability density functions.[12] This distance measure is given by:

$$d = (\sum_{\mathbf{r}} \iint (\rho_A(g_1,g_2,\mathbf{r}) - \rho_B(g_1,g_2,\mathbf{r}))^2 dg_1,dg_2)^{1/2}, \qquad (6)$$

in this case, g_1 and g_2 are the grey levels at pixels 1 and 2 within the images; and **r** is the vector separation between locations 1 and 2. The summation is over a finite set of vectors **r**. The vector is considered to be finite because the images consist of a finite set of pixels, the spacing of which helps to determine a lower bound. Going back to equation (2) we see that the 2P-PDF is equivalent to the product of the two 1P-PDFs, for the case of large **r**. Consequently, because the 1P-PDFs are all the same, all of the corresponding terms are eliminated, thus setting an upper bound for **r**. Additionally, the upper bound could be determined by the image size. Inaccuracies may result, in this case, in the estimation of both the 2P-PDFs and the associated distance d. In any case, the need to select an optimal parameter for **r** in order to calculate the 2P-PDF is alleviated.[14,15] If ρ_A and ρ_B represent the 2P-PDFs of two images A and B, the distance between the two images is estimated. If ρ_A and ρ_B represent the ensemble 2P-PDFs of two texture classes, the distance between the two classes is estimated.

2.5 Normalization of 2P-PDF

We have hypothesized that prior to the determination of a distance measure, the normalization of the 2P-PDF of a texture image is necessary when performing texture characterization or classification. Normalization plays a critical role because variations in the 1P-PDF of a texture cause variations in the associated 2P-PDF. For example, any comparison between textures without initial normalization would be equivalent to comparing two pictures of the same scene or object acquired in different light settings. That is to say, if we take a picture of a rock at noon and then retake the same picture later in the evening, the pictures are the same in structure, but the information readily available for the 2P-PDFs would vary greatly due to the difference in the greyscale. This concept is illustrated in Figure 5 A-D. A distance measure between the 2P-PDFs of the two pictures would yield results that infer that the two textures have different structures. This would lead to a classification of the two images as members of different groups. It is thus necessary to normalize the two-point probability density function to remove any potential contributions from the one point probability density function of a random process, in order to be able to compute a distance measure with results that are meaningful.

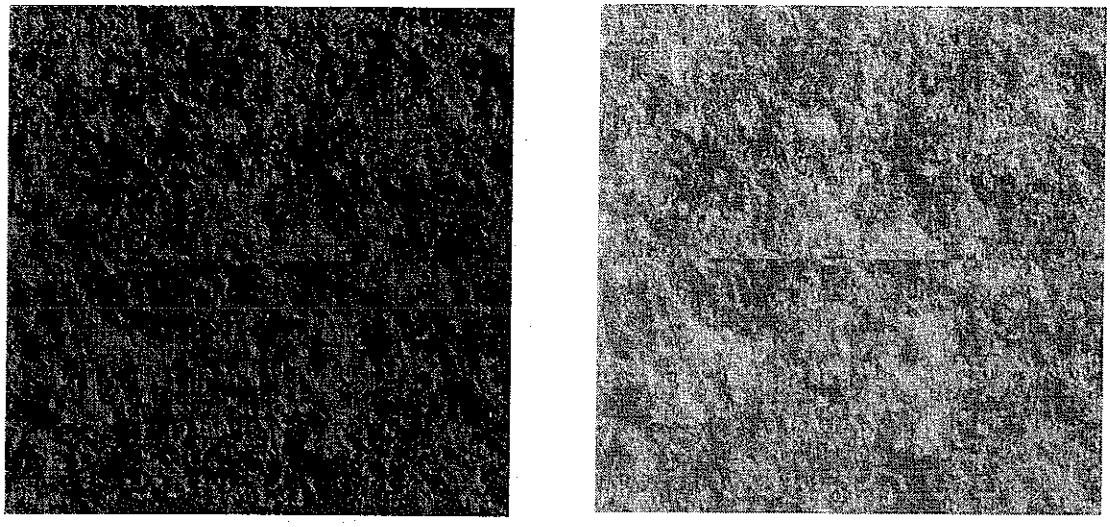

(A) (B)

Figure 5. To depict the need for normalization prior to the determination of a distance measure, the grey level values of one rock texture sample has been scaled to 2 different ranges: (A) A rock texture scaled from 0 to 150 grey levels, and (B) the same rock texture scaled from 105 to 255 grey levels.

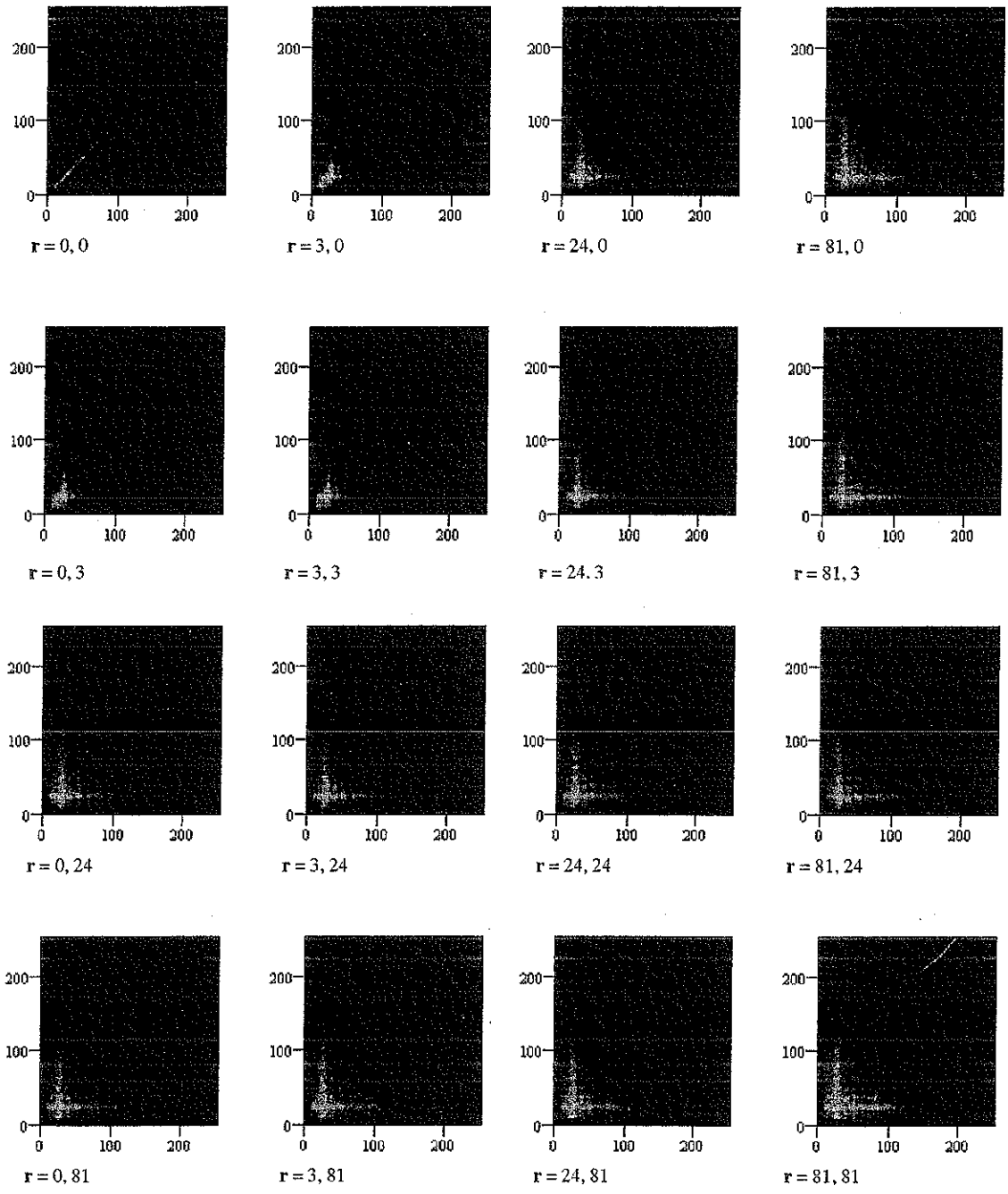

Figure 5C The complete 2P-PDF of the rock texture scaled from 0 to 150, with **r** values ranging from $\mathbf{r} = \mathbf{r}(0,0)$ to $\mathbf{r} = \mathbf{r}(81,81)$ is shown. The brighter the colors, the higher the frequency of occurrence of a pair of grey levels. This figure shows that as r increases, the shape of the 2P-PDF becomes more rotationally symmetric, thus reflecting the lower correlation between grey levels.

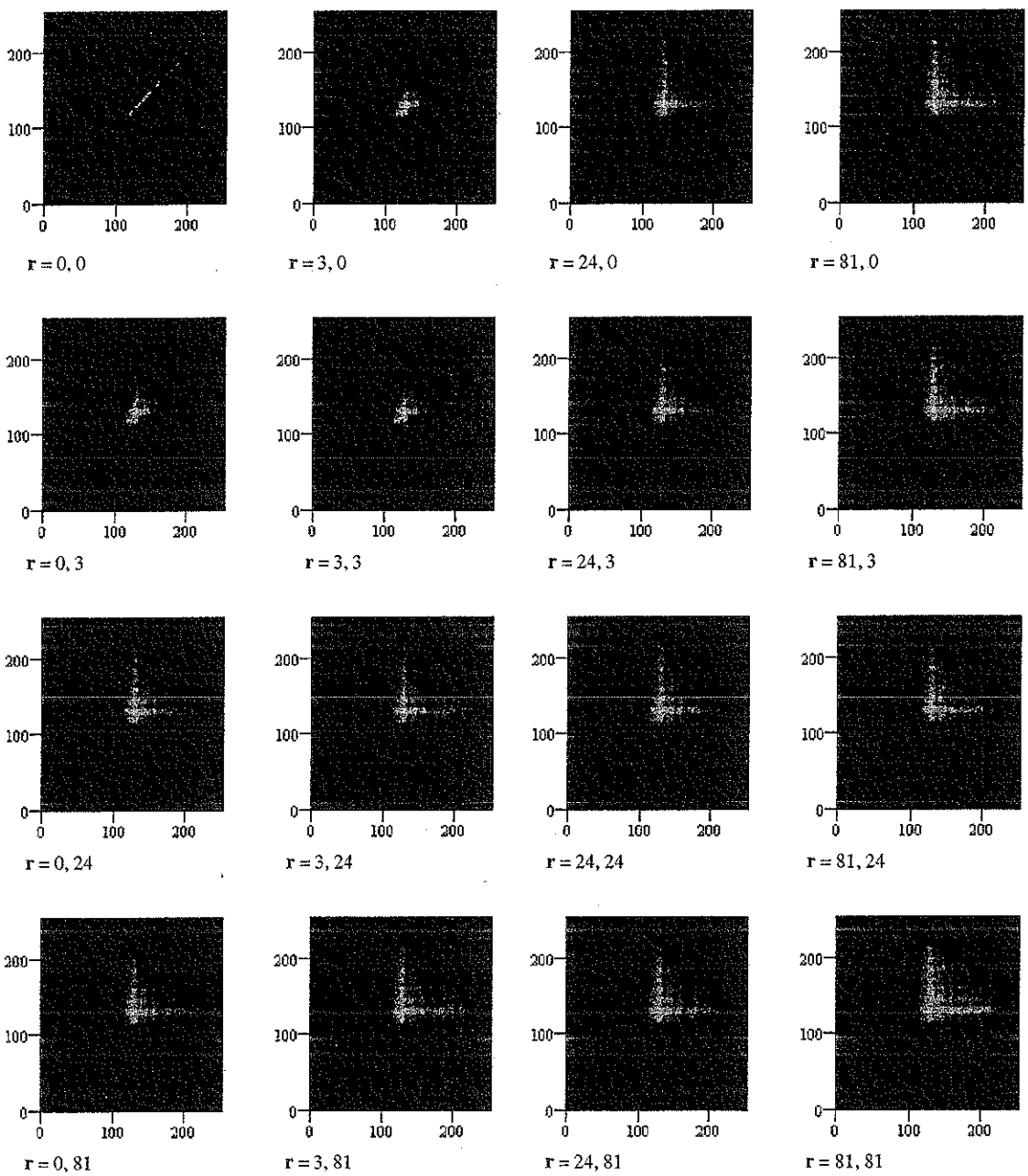

Figure 5D The complete 2P-PDf of the rock texture scaled from 105 to 255, with **r** values ranging from **r** = **r**(0,0) to **r** = **r**(81, 81) is shown. Compared to Figure 5C this figure shows how a shift in the overall greyscale causes a shift in the associated 2P-PDFs.

CHAPTER 3 – EXPERIMENTAL METHODS

3.1 Image simulation

To investigate the impact of the normalization of second-order statistics when performing texture characterization, three different normalization methods have been implemented. In doing so, we have generated a total of four different sets of images each relating to a different type of normalization: unmodified images (or no normalization); scaled images; and images whose histograms have been matched to either an image with a uniform distribution of grey levels referred to henceforth as a uniformly distributed white noise image, or an image with a normal (Gaussian) distribution.

3.1.1 Unmodified images

We considered four texture classes: rock, grass, granite, and residual mammogram texture. The residual mammogram texture will thus be referred to as the residue texture. The first three texture images were acquired from Brodatz's texture atlas.[16] The residue texture was formed by blurring a mammographic texture with a Gaussian distribution having a standard deviation of six pixels. The resulting spatially varying image was subtracted from the original mammogram image, thus producing the residue texture image.[17]

From these sample textures, the unmodified images are generated by utilizing the texture synthesis framework described in Chapter 2. A total of 100 images were

synthesized, 25 for each texture class. The 25 synthesized rock images are produced from the combination of the rock sample texture and twenty-five different realizations of

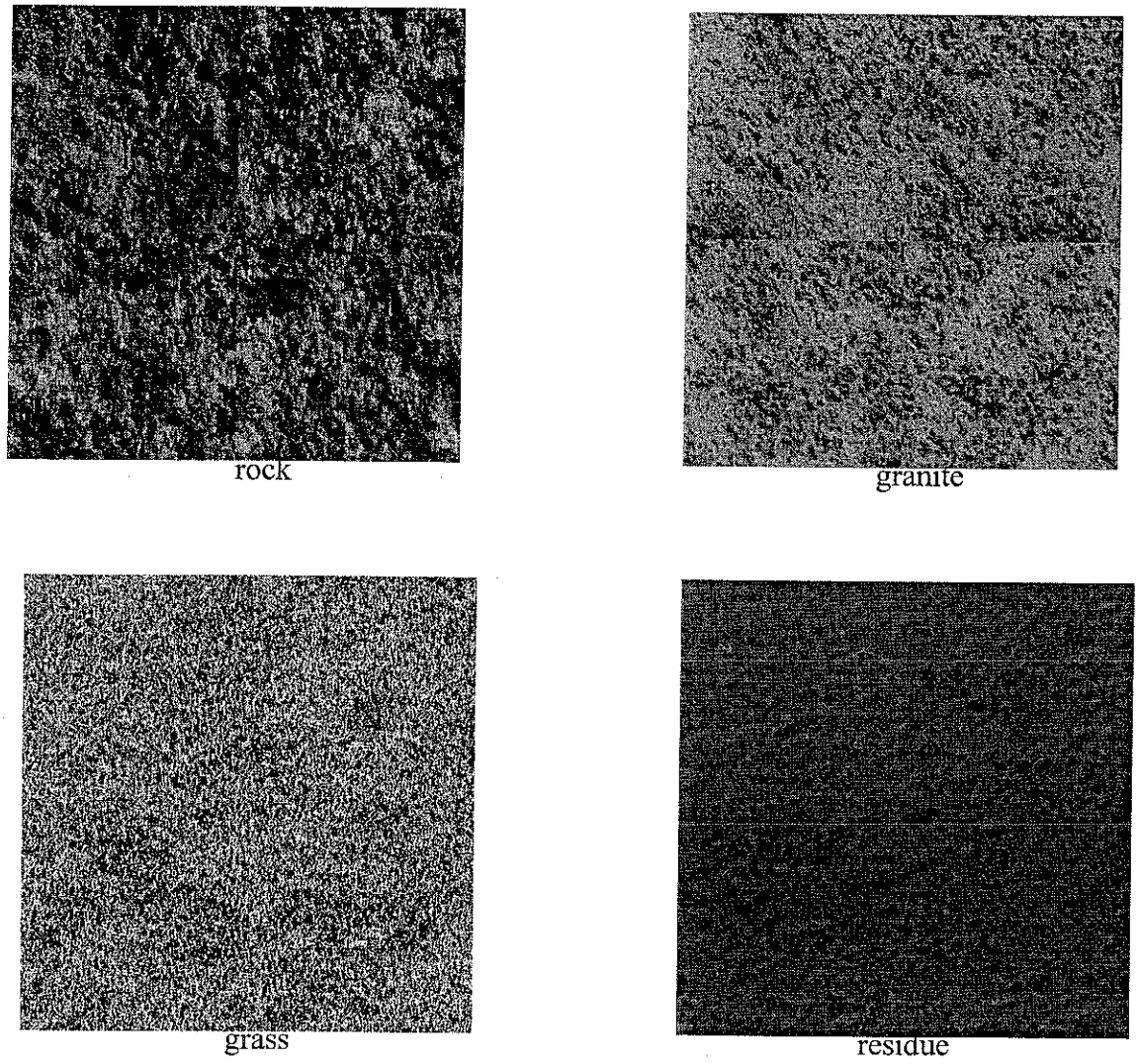

Figure 6 Four texture samples are shown: the "rock", "granite", "grass", and "residue" textures. For each texture four images were assembled to form each texture image. For example in the upper left quadrant of the rock image is the original sample texture. The three remaining quadrants are synthesized samples of the rock texture. Similarly, this applies to the granite, grass and residue textures.

uniformly distributed white noise images. The other 75 texture images, from the grass, granite, and residue classes, are synthesized in the same fashion. Each synthesis employs a different realization of a uniformly distributed white noise image. Samples of the syntheses can be seen in Figure 6. The 100 unmodified images provide the basis for the scaled and histogram matched texture images.

3.1.2 Linearly scaled images

For the case of the scaled images, a weighting function is applied to each image. The grey level values of each image are linearly scaled from 0 - 255. This is done by applying a weighting equation to the specified image, given by

$$\mathrm{OutputImage} = (\mathrm{InputImage} - \mathrm{MinIn}) \times \frac{\mathrm{MaxOut} - \mathrm{MinOut}}{\mathrm{MaxIn} - \mathrm{MinIn}} \qquad (8)$$

where InputImage is the array of pixels that makes up the input image, and OutputImage is the array of pixels that makes up the output image. MinIn and MaxIn are the minimum and maximum grey level values of the input image, respectively. The maximum and minimum grey level value of the output image in our case, MaxOut and MinOut, equal 255 and 0, respectively. This type of normalization may experience problems with noisy images, because of possible grey level outliers. If this form of scaling was retained, this issue may be addressed with the application of some form of filtering (e.g. a median filter) before the scaling is applied.

3.1.3 Histogram-matched images

We shall now normalize the 100 unmodified images by applying the histogram matching process to each of the texture images. The purpose for utilizing histogram matching is that it offers a method for the modification of the one-point probability density function of all the images to some desired form. An exact histogram matching procedure was applied to create the two normalized sets of textures. Specifically, the sort-matching algorithm was employed to produce images whose histograms are matched exactly to the histogram of a model image.[18] The model image will be either a uniform white noise or a Gaussian noise image.

3.1.3.1 Uniformly distributed grey level images

The second set of images was histogram matched to a uniformly distributed white noise image. The 512 x 512-pixel array white noise image was generated with the use of a random number generator that produced a uniform distribution of numbers ranging from zero to one.

3.1.3.2 Gaussian distribution grey level images

The third set of texture images was matched to a Gaussian distribution noise image. The Gaussian distribution was produced with the use of a random number generator, RandomN, which generates a normal distribution of numbers centered at zero, with a standard deviation of one. For our purpose we instituted a Gaussian distribution,

$$\text{Gauss} = 128 + \text{RandomN} * (128/3). \qquad (9)$$

Gauss is a distribution with a mean value of 128 and a standard deviation of 128/3. This value was chosen in order to allow for an untruncated Gaussian.

3.2 Distance measurement

The calculation of the distance measure between two 2P-PDFs requires that the determination of the 2P-PDFs of the textures considered be followed by the application of the distance algorithm. Beginning with the 2P-PDF, we first determined the co-occurrence of two pixels of grey levels g_1 and g_2, which are separated by a vector distance $\mathbf{r} = \mathbf{r}(x, y)$.

A relative frequency method was employed to estimate the 2P-PDF. This method takes two copies of the same image, let's say image A in this case, and while holding one image stationary shifts its copy by a vector distance **r** from it's originating position. This is done to find the co-occurrence of the grey levels for each pixel in the overlapping area, which is equivalent to determining the number of occurrences of specific grey level pairs within the same image when separated by a distance vector **r**. This process is illustrated in Figure 7. The sum of the elements of the acquired grey level distribution array or 2P-PDF was then normalized to 100. Similarly this process was applied to a second image, B. We next determined d^2, the squared difference between the two normalized 2P-PDFs. The global distance measure between the 2P-PDFs was obtained by summing over the **r** values and taking the square root, as expressed in Eq. (6).

Based on symmetry and computational time, we only sum over the values of **r** such that repetitions of specific **r** values are left out. Recognizing that **r** = **r**(x,y) is equivalent to **r** = **r**(-x,-y) we avoid summing over equivalent values of **r**.

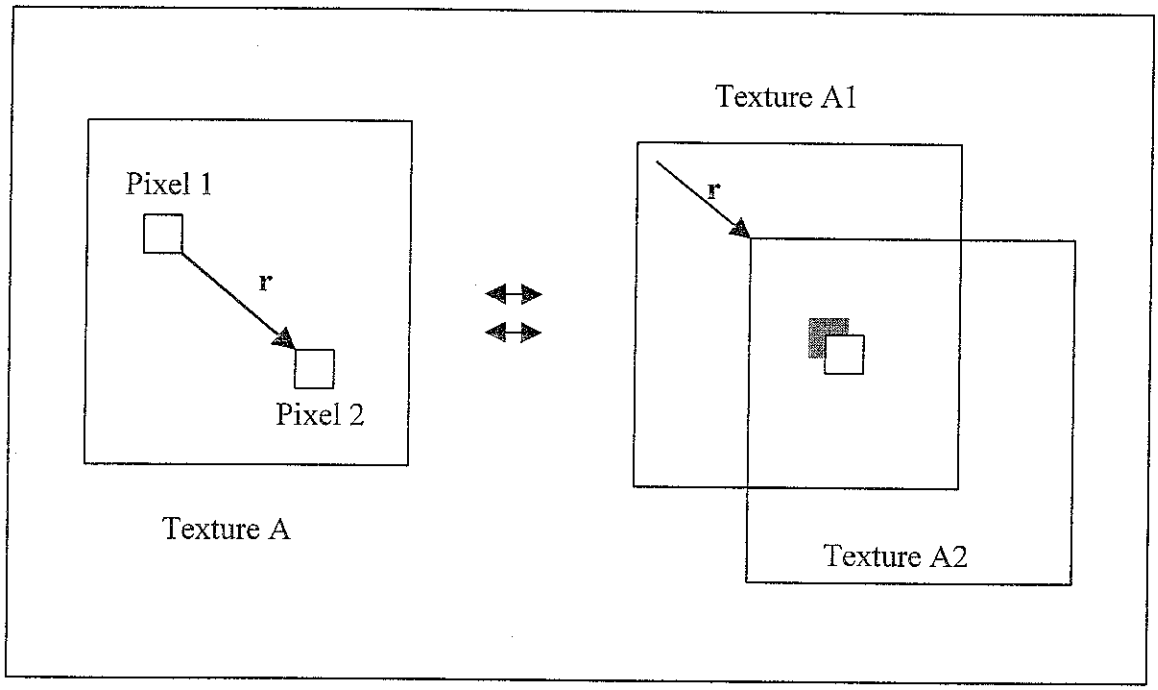

Figure 7 The relative frequency method used to estimate the 2P-PDF is illustrated, for a given **r** value. To determine the co-occurrence of grey level pairs within an image, two copies of an image, A1 and A2, are made. A2 is shifted, by some vector **r**, from the origin of A1. In the overlapping area between the images, pairs of grey levels are automatically formed. The frequency of occurrence of various pairs of grey levels within the overlapping area provides the 2P-PDF of image A, for a given **r**.

CHAPTER 4 - RESULTS

We shall present results of distances computed within and between the four classes rock, grass, granite, and the residue texture. Distance measures within a class, also referred to as intra-class distances, should offer small variations in distances, while distance measures between classes, also referred to as inter-class distances, should furnish larger variations in the distances. More specifically, for an effective measure of class separability it is necessary that the inter-class distances be in agreement with Eq (4), where the inter-class distance is larger than the sum of the radii of the two individual classes.

Figure 8 shows the computation of intra-class distances, that is the distribution of distances between all possible combination of pairs of single image 2P-PDFs within a group. The distances are plotted as a function of the frequency of occurrence of a distance value. The three plots within Figure 8 apply to images that are linearly scaled, matched to a uniform distribution, and matched to a Gaussian distribution, respectively. It can be seen that all of the intra-class distances are relatively small in value as expected, where small will in fact be measured relative to typical inter-class distances.

With respect to inter-class distances, although the distribution of distances between pairs of images, each from one class, may yield an overlap between various pairs of classes considered, this is not an absolute sign of there being no discrimination between classes. It is necessary to determine if the distance between classes is equivalent

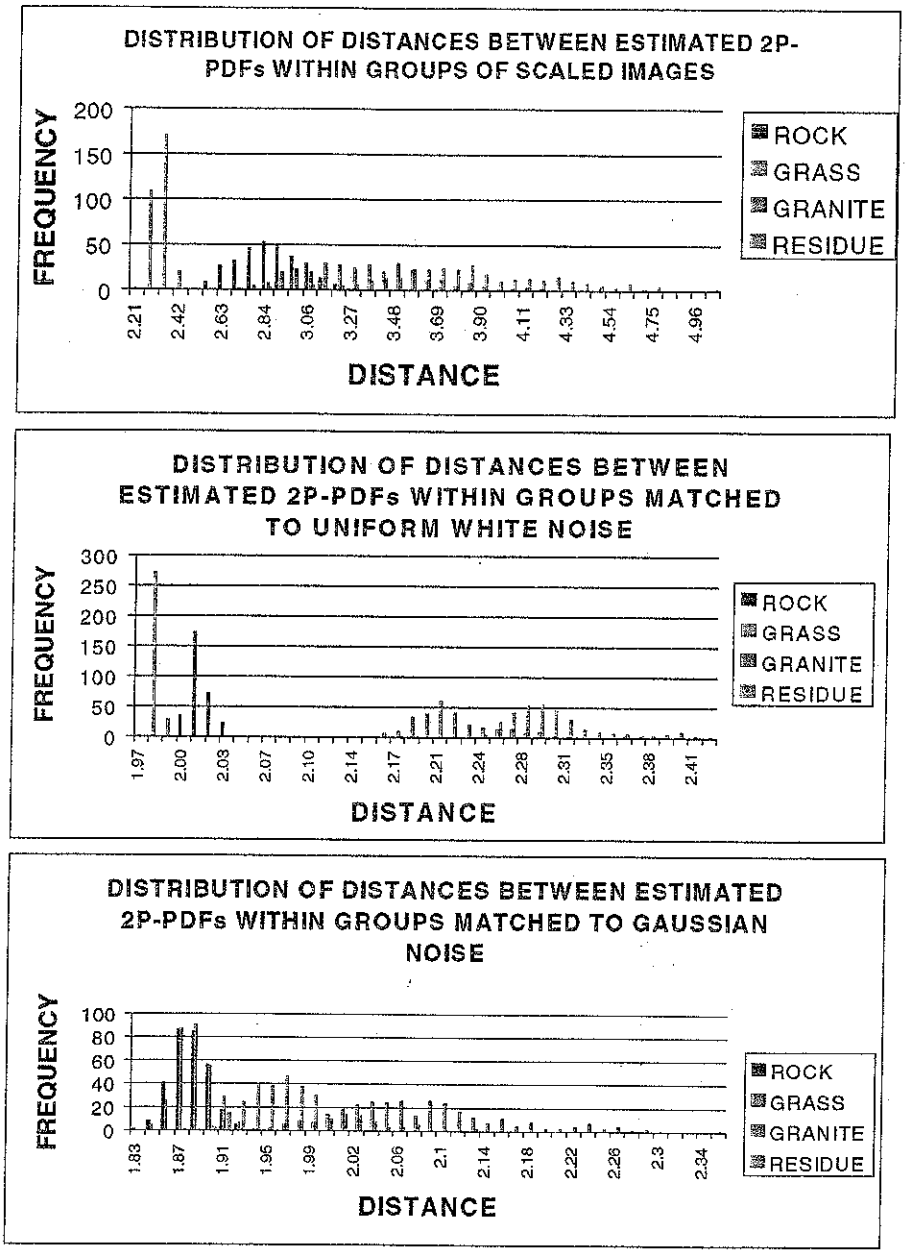

Figure 8 The distribution of distance measures between estimated 2P-PDFs within groups is shown. The 2P-PDF is estimated for each of the images within a texture class. The distance measure between the 2P-PDFs of all the possible pairs of image combinations within a group are made. These distance measures are then plotted here as a distribution of distance as a function of frequency of occurrence. The first plot being for linearly scaled images, the second plot for images that have been matched to a uniform distribution, and the third for images that have been matched to a Gaussian distribution.

to, larger than, or smaller than the sum of the within class radii of the two classes in question.

Figures 9, 10, and 11 represent the distribution of inter-class distances. The distribution plots for Figure 9 are created by estimating the 2P-PDFs of each image within the four texture ensembles. Taking two ensembles at a time the distance measure between the 2P-PDFs of the images from the different groups are calculated, for all possible image pair combinations. The distributions are then plotted as a function of frequency. Plots A, B, C, and D are made with respect to granite, grass, residue, and rock, respectively. Figure 10 illustrates the distribution of distances between groups that have been matched to a uniform grey level distribution. Figure 11 depicts the distribution of distances between groups that have been matched to a Gaussian distribution. Both Figures 10 and 11 are created utilizing the same method as Figure 9. The amount of overlap of the distance distributions varies in each of these figures, and is more or less pronounced dependent upon the method of normalization utilized. We shall now examine each case.

4.1 Distribution of distance measures between groups: Linearly scaled images

This form of normalization offers a good but sub-optimal class separability. This is due to the closeness of the value of the distance between rock and grass, shown on the x-axis of Figures 9 B and D, and the sum of the radii of the two classes, given in Table 1. However in spite of the small value encountered, because $d_{ROCK\text{-}GRASS}$ is larger than the sum of the two classes' radii we are able to discriminate between the classes. Other

distances found between classes and reported in Figure 9 are well above the sum of the radii of the corresponding classes. However, it is likely that for cases where the texture images are less visually discriminable, this method will not be able to provide effective class separability.

4.2 Distribution of distance measures between groups: Histogram-matched images to a flat distribution

This process provides a poor result for class separability. It neither satisfies the criteria for effective texture classification given by Eq. (4), nor provides a distinct separation between any pair of the texture classes. This can be confirmed by comparing the distance values of Figure 10 and the results of Table 2. We hypothesize that this poor performance is partially due to the fact that the broad range of grey levels utilized in this method is unable to provide an accurate estimate of the 2P-PDF. If so, this could have been alleviated by the use of texture images of a larger size, however, the texture images used were intentionally kept at a size of 512 x 512-pixels for comparison purposes.

4.3 Distribution of distance measures between groups: Histogram-matched images to a Gaussian distribution

This method of normalization provides effective class separability for textures, as shown in Figure 11 and Table 3. This method offers the highest level of discriminability between groups. The distance measures provided when using this form of histogram matching allow for a specific range of distance measure distributions between any two

classes. The lack of overlap between any of the distance measures and the large values of d, except for the distance between granite and rock, compared to the individual spread of the classes shows the potential of this technique for efficacy of classification. Although small between class distances are observed, this method remains the most potentially effective because of the ability to optimize the standard deviation of the Gaussian distribution, which would potentially allow an even higher level discriminability between classes.

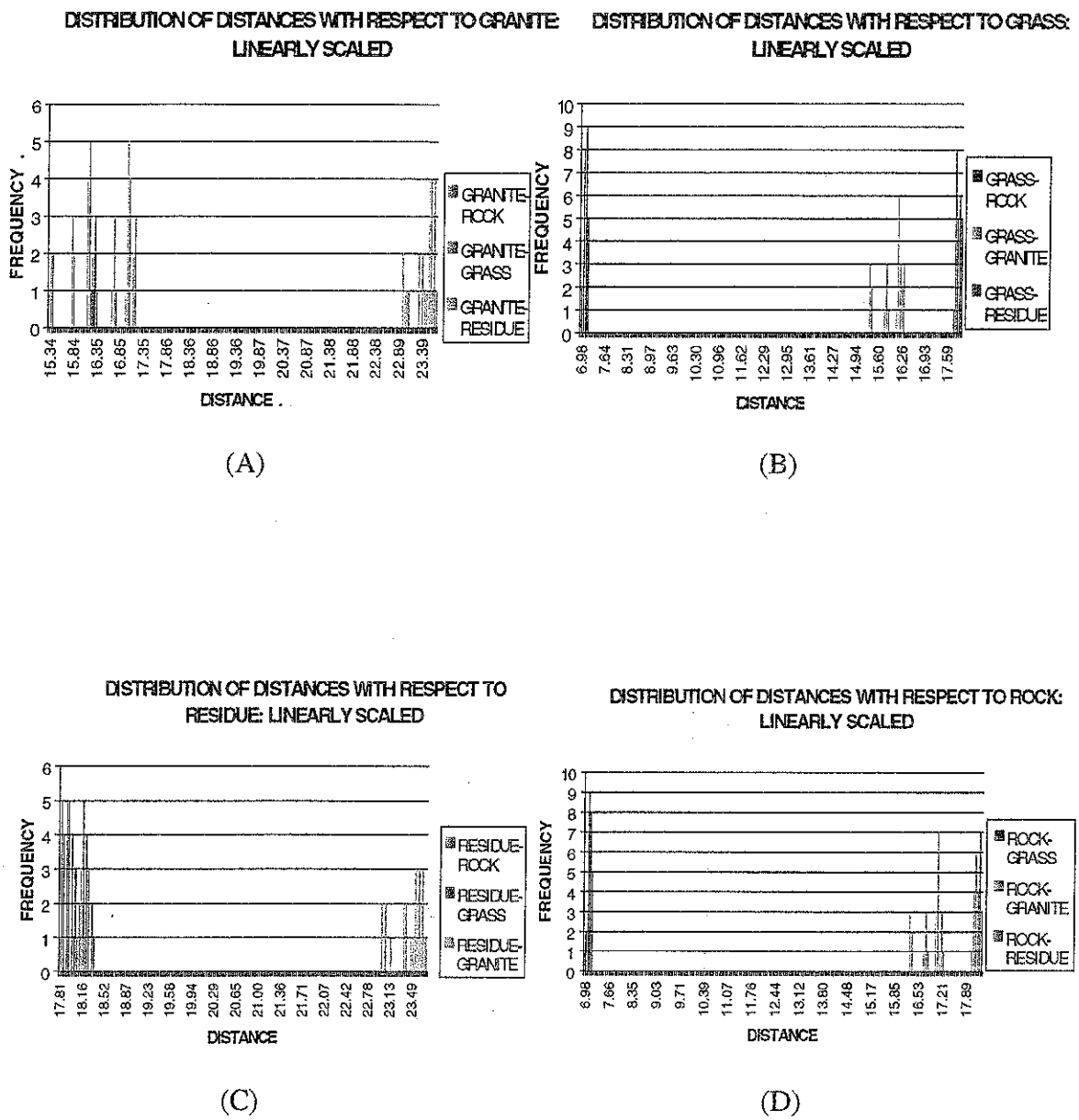

Figure 9 The distribution of distances between the 2P-PDFs groups that have been linearly scaled with respect to (A) Granite, (B) Grass, (C) Residue, (D) Rock is shown. These plots are created by estimating all of the 2P-PDFs for each of the individual images within the four groups of images that have been linearly scaled. Utilizing two ensembles of textures at a time, the distance measures between the 2P-PDFs of images from two different groups are calculated, for all possible image pair combinations. The distribution of distance measures is plotted here as a function of the frequency of occurrence of the distance values. Each plot is with respect to a particular texture group.

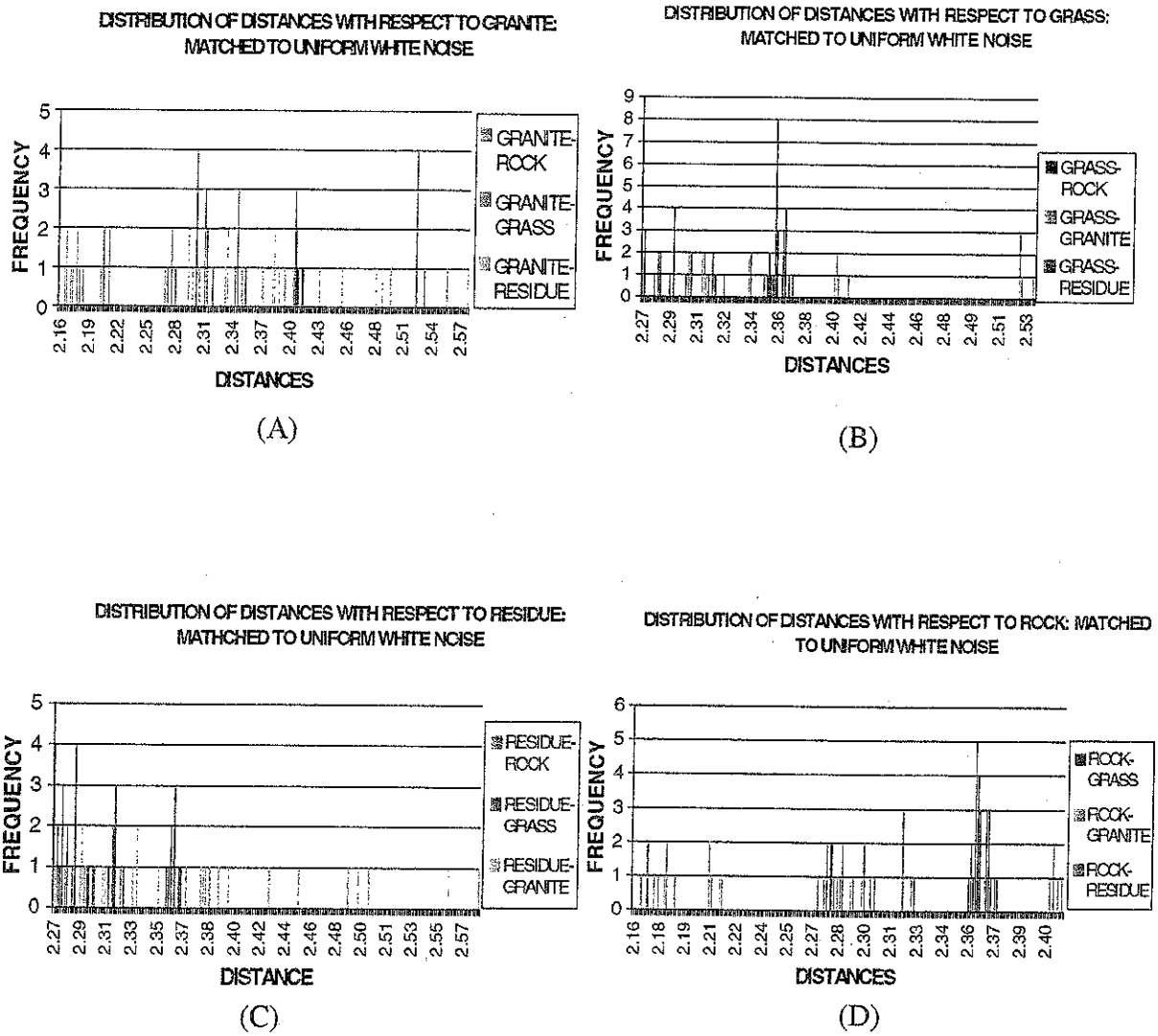

Figure 10 The distribution of distances between groups that have been matched to uniformly distributed white noise with respect to (A) Granite texture, (B) Grass texture, (C) Residue texture, and (D) Rock texture is shown here. These plots are created by estimating all of the 2P-PDFs for each of the individual images within the four texture groups that have been matched to a uniform distribution. Utilizing two ensembles of textures at a time, the distance measures between the 2P-PDFs of images from two different groups are calculated, for all possible image pair combinations. The distribution of distance measures is plotted here as a function of the frequency of occurrence of the distance values. Each plot is with respect to a particular texture group.

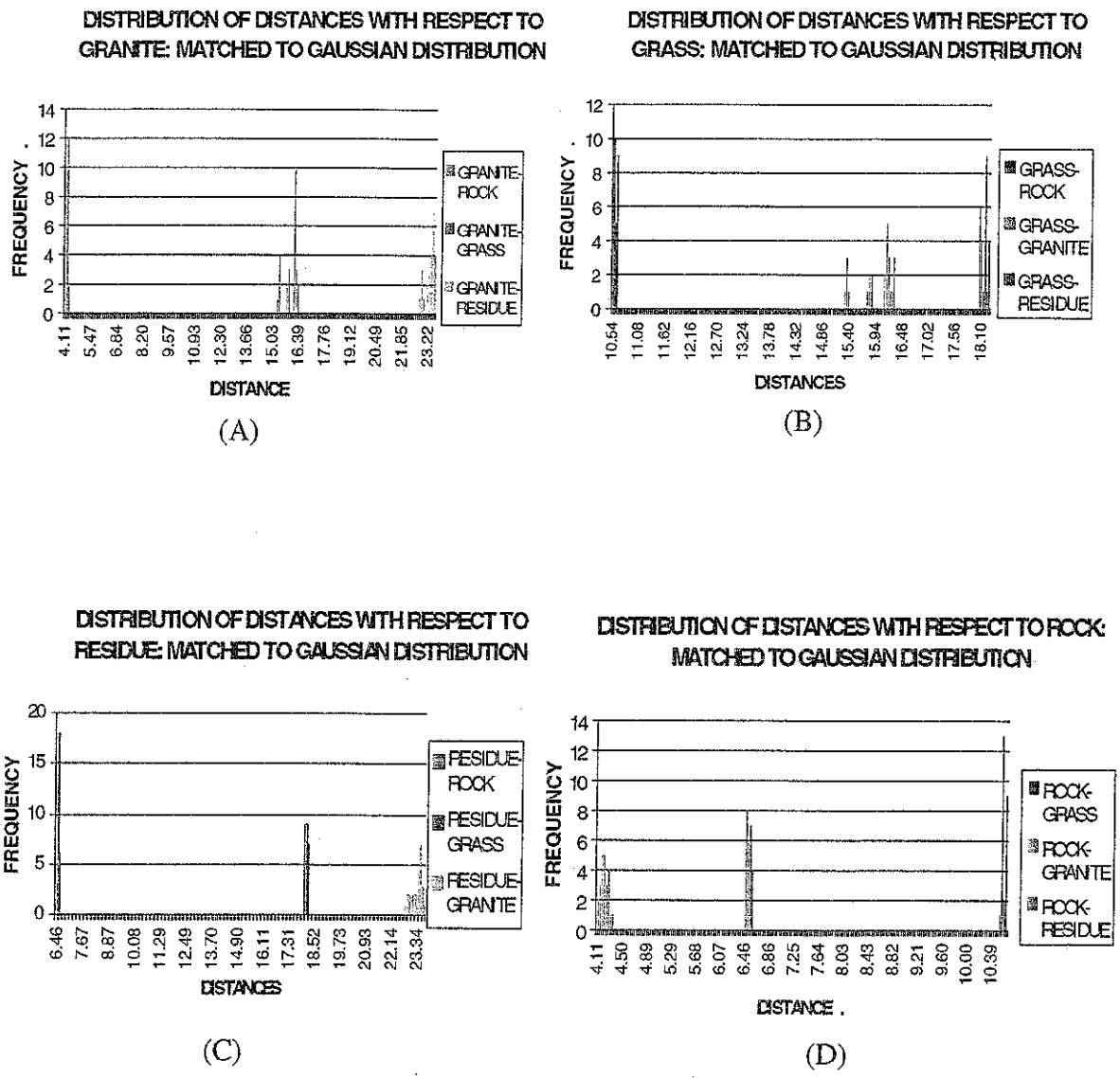

Fig 11. Distribution of distances between groups that have been matched to a Gaussian distribution with respect to (A) Granite texture , (B) Grass texture, (C) Residue texture, and (D) Rock texture. These plots are created by estimating all of the 2P-PDFs for each of the individual images within the four texture groups of images that have been matched to a Gaussian distribution. Utilizing two ensembles of textures at a time, the distance measures between the 2P-PDFs of images from two different groups are calculated, for all possible image pair combinations. The distribution of distance measures is plotted here as a function of the frequency of occurrence of the distance values. Each plot is with respect to a particular texture group.

Texture A	Texture B	$r_{.95}^{A} + r_{.95}^{B}$
ROCK	GRANITE	6.788
ROCK	GRASS	5.38
ROCK	RESIDUE	7.498
GRASS	GRANITE	6.1
GRASS	RESIDUE	6.811
GRANITE	RESIDUE	8.218

Table 1 The sums of the radii of texture pairs, for scaled images, are listed here. The radius of each ensemble of textures is determined by first calculating the ensemble average 2P-PDF, by estimating the 2P-PDFs of each of the images within an ensemble. Utilizing all of these 2P-PDFs an average 2P-PDF is computed. The distances between the average 2P-PDF of a class and the individual textures within the class are then computed, thus showing the distribution of distances with respect to the average 2P-PDF. This distribution is also known as the radius of a texture class or the spread of textures within a class.

Texture A	Texture B	$r_{.95}^{A} + r_{.95}^{B}$
ROCK	GRANITE	4.398
ROCK	GRASS	4.001
ROCK	RESIDUE	4.357
GRASS	GRANITE	4.352
GRASS	RESIDUE	4.311
GRANITE	RESIDUE	4.708

Table 2 The sums of the radii of texture pairs, for images matched to a uniform distribution, are listed here.

Texture A	Texture B	$r_{.95}^{A} + r_{.95}^{B}$
ROCK	GRANITE	4.098
ROCK	GRASS	3.797
ROCK	RESIDUE	3.926
GRASS	GRANITE	4.104
GRASS	RESIDUE	3.931
GRANITE	RESIDUE	4.233

Table 3 The sums of the radii of texture pairs, for images matched to a Gaussian distribution are listed here.

CONCLUSION

A method of texture characterization based on the complete second-order statistics of the associated random process was proposed. The necessity for the normalization of the second-order statistics was presented. Three methods of normalization, linear scaling, and histogram matching to uniform, and Gaussian distributions were investigated.

Three different sets of results were obtained for the case of texture characterization employing visually discriminable, synthesized ensembles of images. Good, but sub-optimal class separability was yielded for linear scaling. Histogram matching to a uniform distribution produced poor class separability. Higher overall class separability was yielded with the utilization of histogram matching to a Gaussian distribution.

Given this encouraging result on synthesized texture ensembles that can be discriminated visually, future research will include natural texture classes that differ more subtlely. Furthermore, future research will aim to establish whether this finding, for histogram matching to a Gaussian distribution, extends to medical texture data sets, by determining a theoretical normalization function that predicts maximum class separability over typical data sets (e.g. ultrasound liver images or MR images of bone).

LIST OF REFERENCES

1. H. Barrett, J. Yao, J. Rolland, and K. Meyers, "Model observers for assessment of Image quality," Proc. Natl. Acad. Sci. **90**, 9758 –9765 (1993).

2. J. Rolland, (1990) Ph.D. dissertation (Univ. of Arizona, Tucson).

3. J. Rolland, H. Barrett, "Effect of random background inhomogeneity on observer detection performance," J. Opt. Soc. Am., (1992).

4. E. Cargill, (1989) Ph.D. dissertation (Univ. of Arizona, Tuscon).

5. R. Haralick, "Statistical and structural approaches to texture,", Proc. IEEE **67**(5), 786-804 (1979).

6. J.W. Goodman, *Statistical Optics*, Chap. 2, Wiley-Interscience, New York (1985).

7. B. Julez, "Visual pattern discrimination," IRE Trans. Inform. Theory **8**(2), 84–92 (1962).

8. J. Byng, M. Yaffee, G. Lockwood, L. Little, D. Tritchler, and N. Boyd, "Automated analysis of mammographic densities and brest carinoma risk," Cancer **80**(1), 66-74 (1997).

9. F.G. Stremler, *Intro to Communication Systems*, Chap. 4.2, Addison-Wesley, Reading, MA (1990)

10. F. Bochud, F. Verdun, C. Hessler, and J. Valley, "Detectability in radiological images: the influences of anatomical noise," Medical Imaging 1995: Image Perception, H.L. Kundel, ed., Proc. SPIE **2436**, 156-165 (1995).

11. J. Rolland, A. Goon, and L. Yu, "Synthesis of textured complex backgrounds," Proc. SPIE **37**(7), 2055-2063 (1998).

12. Goon and J. Rolland, "Texture classification based on comparison of second-order statistics I: 2P-PDF estimation and distance measure," J. Opt. Soc. Am. A, July 1999 (in press).

13. Papoulis, *Probability, Random Variables, and Statistical Processes*, McGraw-Hill, New York (1991).

14. A. Tremeau, J. Bousigue, B. Laget, "Co-occurrence shape descriptors applied to texture classification and segmentation," in *Machine Vision Applications in Industrial Inspection*, R. Rao, N. Chang, eds., Proc. SPIE **2665**, 135-147 (1996).

15. R. Mia, M. Loew, K. Wear, R Wagner, B Garra, "Quantitative ultrasound tissue characterization using texture and cepstral features," in *Medical Imaging: Image Processing*, K. Hanson, ed., SPIE **3338**, 211-219 (1998).

16. P. Brodatz, *Textures: A photographic album for artists and designers*, Dover Publications, New York (1966).

17. J. Rolland, R. Strickland, "An approach to the synthesis of biological tissue," Optics Express **1**(13) (1997).

18. J. Rolland, L. Yu, C. Abbey, V. Bo, and B. Bloss, "An optimal algorithm for histogram matching: application to texture synthesis" (in press).

19. Goon and J. Rolland, "Texture classification based on comparison of second-order statistics II: Noise and 2P-PDF", J. Opt. Soc. Am. A (In press).

20. K. Myers, J. Rolland, H. Barrett, and R. Wagner, "Aperture optimization for emission imaging: effect of a spatially varying background.", J. Opt. Soc. Am. A (1990).